Photoelectrochromic devices with cobalt redox electrolytes

Photoelectrochromic devices with cobalt redox electrolytes

Alexandros Dokouzis*, Federico Bella**, Krystallia Theodosiou*, Claudio Gerbaldi**, George Leftheriotis*

*Renewable Energy and Environment Lab, Physics Department,
University of Patras, Rion, 26500, Greece
Tel: +30 2610 996793; e-mail: glefther@physics.upatras.gr

**Group for Applied Materials and Electrochemistry (GAME Lab), Department of Applied Science and Technology (DISAT), Politecnico di Torino, Corso Duca degli Abruzzi 24, 10129 – Torino (Italy)
Tel: +39 011 0904643, e-mail: federico.bella@polito.it

***Keywords*:** Photoelectrochromic, Cobalt electrolyte, Titania, Tungsten oxide, ZnS barrier.

Abstract

In this work, the use of cobalt redox electrolytes in partly covered photoelectrochromic devices is investigated experimentally for the first time. The fabricated devices consist of a conductive glass photoanode coated with an electrochromic WO_3 film of optical quality, including a mesoporous TiO_2 layer (sensitized by the MK2 organic dye) that covers 20% of the device area. The liquid electrolyte is composed of 0.22 M $Co(II)(bpy)_3(PF_6)_2$, 0.5 M $LiClO_4$ and 0.5 M 4-tert-butylpyridine. A platinized conductive glass cathode completes the cell set-up. The fabricated devices are almost transparent in the bleached state with a T_{lum} value above 50%. They exhibit coloration speeds in the order of minutes, with a maximum contrast ratio of 2.9:1 after 21 min of illumination at 1000 W m^{-2} under open circuit conditions (OC), and highly reversible to fully bleached state in short circuit conditions. They provide a maximum measured power conversion efficiency of 0.28 % due to limitations imposed by conflicting requirements of the photovoltaic and electrochromic elements, which is nonetheless sufficient to drive the coloration process. Since only the reduced specie Co^{2+} is present, initial illumination under OC for 3 min at 1000 W m^{-2} is necessary, prior to measurements, to oxidize Co^{2+} to Co^{3+} through the dye regeneration process in the electrolyte. The higher recombination losses of the $Co^{2+/3+}$ redox shuttle compared to I^-/I_3^-, which lead to a considerable reduction in coloration depth 20 days post fabrication due to loss of photoelectrons at the WO_3/electrolyte interface, are suppressed by the use of a 35 nm thick ZnS barrier deposited on top of WO_3. Remarkably, it results in a stabilized contrast ratio of 1.5:1, 23 days post fabrication. In addition, the color coordinates of the present devices resemble those of typical electrochromics: they exhibit blue coloration, as a result of the lack of the absorbing iodine in the electrolyte that produces a green tint.

Introduction

In recent years, building integrated photovoltaics and smart windows have gained considerable attention by the international scientific community, due to their promising prospects in terms of energy production from renewables and significant energy savings [1, 2], which pave the way to the realization of next-generation sustainable, smart, energy efficient buildings [3].
Photoelectrochromic windows (PECs, hereafter) are an emerging technology in this field that could combine optimally the aforementioned functionalities into one single device [4]. Actually, PECs usually integrate a dye

sensitized solar cell (DSSC, hereafter) with an electrochromic device (EC, hereafter), so that the former provides the electrical power required by the latter to change autonomously its transparency in response to the prevailing environmental conditions. PECs are still at their infancy, and many issues remain to be solved (*viz.*, performance optimization and stability in real operating conditions) for their exploitation in real life applications [4]. Although a multitude of different architectures have been proposed by the scientific community [4], there is still no consensus as to the optimum design and combination of materials.

In this respect, bringing the DSSC technology to the next maturity phase is expected to be beneficial also to PECs. One of the recent advances in DSSCs is the use of alternative redox couples to the "standard" I^-/I_3^-, with the most successful one being $Co^{2+/3+}$. The main advantage of the cobalt based shuttles is their lower redox energy levels as compared to I^-/I_3^-, that permit an increase of the resulting open circuit voltage to above 0.8 V [5, 6]. Furthermore, with the use of cobalt redox couples, light absorption by triiodide up to 430 nm is avoided, as well as the corrosiveness of I^-/I_3^- towards sealing materials [5]. On the other hand, cobalt based shuttles are more prone to recombination losses; as a result, modifications to the DSSC anode are necessary, such as reduction of the thickness of the TiO_2 layer to few micrometers and use of ultra-thin blocking layers [5]. To date, many reports of the use of cobalt in DSSCs can be found in the literature with power conversion efficiencies ranging from a few per cent to about 10 % [7-12], with a record efficiency of 13 % [13]. It is also known that the standard Ru-based sensitizers containing thiocyanate ligands do not perform well with cobalt electrolytes due to the direct interaction between ruthenium dyes and the cobalt redox species, which reduces charge injection from the dyes to the titanium oxide and, in turn, increases the electron recombination process with the cobalt redox species [14]. Thus, in order to reduce recombination losses, the recent research efforts are directed towards the development of novel sensitizers, suitable for the cobalt redox couple [6, 8, 13, 14], and of alternative cobalt compounds with different ligand groups [7, 10].

As regards photoelectrochromic devices, to our knowledge, only two reports can be found in the literature on the use of cobalt electrolytes [15, 16]. In both articles, the electrochromic material was methyl-poly(propylendioxythiophene) (PProDOT-Me), placed at the counter electrode. TiO_2 was used for the photovoltaic element, sensitized by various dyes, and various cobalt compounds were used in the electrolyte. Resulting devices exhibit low transmittance values of 25 and 35 %, respectively, at 550 nm, too low for practical applications [15, 16]. Furthermore, the device reported by Amasawa et al. [15] required an external bias of +1.5 V for coloration. Therefore, these are only preliminary works, and there is a lot of room for improvement in PECs with cobalt electrolytes.

In the present work, the use of cobalt electrolytes in PEC devices having a "partly covered" architecture is presented for the first time. The devices are transparent in the visible region of the spectrum and exhibit considerable transmittance modulation. The use of an ultrathin ZnS barrier layer was found to successfully suppress recombination losses at the WO_3/electrolyte interface. It resulted in remarkably stabilized contrast ratio of 1.5:1 almost one month post fabrication, which enlightens the promising prospects of the newly developed devices for smart energy-saving applications.

2. Experimental

2.1 Photoelectrochromic device operation

The typical layout and operating principles of a partly covered photoelectrochromic device appear in Figure 1. The light absorbed by the dye molecules results in excitation of electrons (step #1 in Figure 1a). Injection of electrons from the excited state of the dye to the TiO_2 conduction band follows (step #2 in Figure 1a). Then, the

electrons diffuse into WO_3. It has been proven experimentally that the coverage of a small percentage of the device surface (15 to 20% of the window total area) with TiO_2 is sufficient for uniform coloration [17]. Li ions intercalate into the electrochromic film (WO_3), in order to offset the negative charge of the electrons, and thus WO_3 changes color from clear to dark blue. Coloration is therefore obtained with the device under open circuit conditions (OC) (see Figure 1a), represented by the following redox reaction:

$$xLi^+ + xe^- + WO_3 \Leftrightarrow Li_xWO_3 \quad (1)$$

The reduction of WO_3 is caused by the change in the valence state of tungsten from W^{6+} to W^{5+} (or even W^{4+}) due to intercalation of electrons and Li^+ (step #3 in Figure 1a). The dye molecules are oxidized by the loss of electrons and can be reduced by cobalt ions resident in the electrolyte (step #4 in Figure 1a) according to the following reaction:

$$S^+ + Co^{2+} \Rightarrow S + Co^{3+} \quad (2)$$

Thus, the dye is "regenerated" and the coloration procedure continues until all Co^{2+} ions are converted into Co^{3+}. Short-circuiting the device causes a flow of electrons from WO_3 through the conductive substrate to the external circuit and into the counter electrode. Therein, platinum catalyzes the reduction of Co^{3+} to Co^{2+} (step #1 in Figure 1b) at a potential of 0.57V versus the normal hydrogen electrode (NHE), [7], in accordance to the following reaction:

$$Co^{3+} + e^- \xrightarrow{(Pt)} Co^{2+} \quad (3)$$

Simultaneously, lithium ions from tungsten oxide return into the electrolyte and bleaching occurs (step #2 in Figure 1b), under a closed circuit condition.

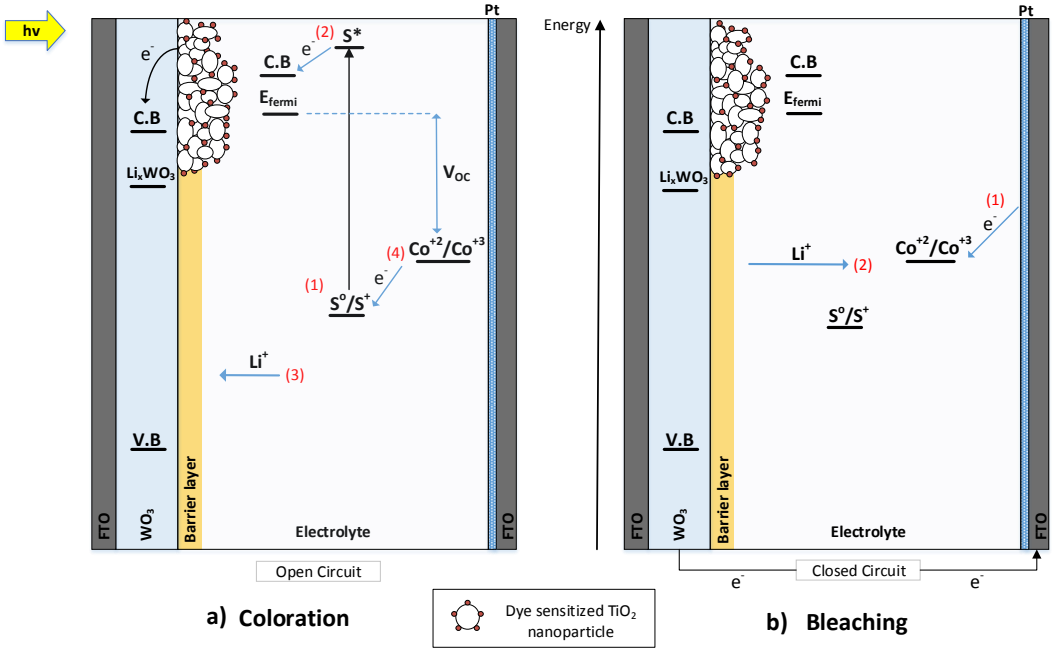

Figure 1: Scheme of "partly covered" PEC device: a) coloration, and b) bleaching process.

2.2 Fabrication of PEC devices

2.2.1. Chemicals

Ethanol, acetone and H_2PtCl_6 were bought by Merck. WO_3 and ZnS were bought from Alfa Aeser. Tritton X was purchased from Fisher Bioreagents and TiO_2 from Degussa. All the other chemicals mentioned hereafter were bought from Sigma-Aldrich. All compounds were used as purchased, without further purification.

2.2.2. Preparation of WO_3 films

WO_3 films were prepared by electron beam gun evaporation, at about 10^{-5} mbar and room temperature in a vacuum chamber that was evacuated using both a mechanical and a turbo-molecular pump. The precursor material was 99.99% pure WO_3 powder. As a substrate, a 4 mm-thick glass coated with a transparent conductive SnO_2:F layer was used (also known as FTO, sheet resistance of 16.7 Ω/sq, 80 % transmittance in the visible, trade name: K-glass). In order to achieve the desirable thickness of films, a quartz controller was used.

Initially, substrates were cleaned with a soft detergent, then ultrasonic bath treatment took place first in ethanol (5 vol% in water) and, then, in acetone (5 vol% in water) solutions. Finally, the substrates were heated at 120 °C for 15 min. As prepared WO_3 films were amorphous, with high optical transparency (≈74%) in the visible range [17, 18] and an average thickness of 600 nm (±15%).

2.2.3. Preparation of ZnS barrier layers

Barrier layers for our devices were prepared by electron beam gun evaporation using the above detailed vacuum chamber. The precursor powder was 99.99% pure zinc sulfide. The thickness of the deposited barrier layers was 35 nm. Like before, a quartz crystal was used in order to achieve the desired thickness. The barrier layer was deposited on top of the tungsten oxide film with use of an appropriate mask to expose a fraction equal to the 80 % of the active area of the device, while the remaining 20 % under the mask was covered by the TiO_2 film.

2.2.4. Preparation of dye-sensitized TiO_2 films

Semiconductor films were prepared by the doctor blade technique. More in detail, a quantity of 2 g of TiO_2 nanoparticles powder (Degussa P25) was hand mortared with 0.5 mL of nitric acid solution (1.5 M). The acidic additive was used to prevent the formation of large aggregates [17, 18, 19]. Distilled water was added under continuous grinding to reach the desirable density value of 1.6 g mL^{-1}. The last step of the preparation of the precursor paste was the addition of a surfactant (Triton-X) so that the spreading of the paste on the FTO/WO_3 was facilitated. Adding Triton-X reduced the surface tension of the paste and homogeneous spreading was achieved [20].

The TiO_2 paste was ground in the mortar for more than 40 min. Next, it was ultrasonicated for additional 20 min in order to further break down large aggregates and improve homogeneity of the paste.

After air drying of the TiO_2 films, calcination at 120 °C for 40 min took place, which served for two purposes: i) burn away the organic components that were used for the preparation of the TiO_2 paste, and ii) improve the electrical connection between the semiconductor and the electrochromic film. The layers were heated at low temperature to avoid re-crystallization of the WO_3 film, which negatively affects the efficient coloration of the device [18, 21]. The TiO_2 film thickness ranged from 3 to 5 μm. Indeed, photoanodes thinner than the 10 μm used with iodine electrolytes are needed in cobalt-based systems, as already demonstrated experimentally [9, 13]

The TiO_2 films were sensitized by dipping into a 3×10^{-4} M solution of MK2 dye in an equivolumetric mixture of toluene-ACN for approximately 6 h. After soaking, the samples were extracted from the solution and thoroughly rinsed with absolute ethanol to remove the excess dye.

2.2.5. Preparation of electrolyte

The electrolyte used in our experiments contained only the reduced Co^{2+} cation, i.e., $Co(II)(bpy)_3(PF_6)_2$, at a molar concentration equal to 0.22 M. In addition, the solution contained $LiClO_4$ 0.5 M as the Li^+ source for the WO_3 system and 4-tert-butylpyridine 0.5 M to enhance the potential. The solvent used was an equivolumetric

solution of acetonitrile and 3-methoxypropionitrile. As regards $Co(II)(bpy)_3(PF_6)_2$ preparation, 1 eq of $CoCl_2 \cdot 6H_2O$ and 3.3 eq of (2,2'-bipyridyl) ligand were dissolved in a little amount of methanol to give a light brown-yellow solution. The solution was left to stir under reflux for 2 h and, then, an excess of tetrabutylammonium hexafluorophosphate ($TBAPF_6$) was added to precipitate the compound. As a last step, the product was filtered, washed with methanol, ethanol and diethylether, dried under vacuum, and used without further purification.

2.2.6. Preparation of counter electrodes (cathodes)

The cathodes were obtained by electrodepositing a platinum film starting from an aqueous solution of H_2PtCl_6 with a concentration of 0.002 M in a three-electrode configuration. Electrodeposition was performed on a Metrohm Autolab S.V (PGSTAT204) potensiostat. SnO_2:F coated glass was used as a working electrode, while a Ag/AgCl electrode and a Pt foil were used as reference and counter electrodes, respectively. Electrodeposition was carried out at a constant voltage of 0.4 V for a duration of 60 s in order to prepare counter electrodes with high transmittance (about 70 %). Finally, as for the counter electrode, two small holes (1 mm diameter) were drilled to the substrate before the electrodeposition in order to facilitate electrolyte filling in the pre-sealed cell [22].

2.2.7. Assembly of devices

The devices under study had dimensions of 3.0 cm × 4.0 cm. The steps of their fabrication can be described as follows: the sensitized anode ($FTO/WO_3/TiO_2$) and the cathode were arranged facing each other but keeping a slight displacement along their longitudinal axis, so that enough space was maintained for electrical contacts. Then, a mask of thermoplastic material (tradename Surlyn by Dyesol, with a thickness of 50 μm) was carefully cut giving the dimensions needed to: i) peripherally seal the device, and ii) create the cavity needed for electrolyte filling. Final assembly and sealing was obtained by using metal clamps and heating at 120 ^oC for 12 min to melt the thermoplastic material. Subsequently, insertion of the electrolyte was performed by pouring the liquid in one hole with the air leaking from the other one. The holes were sealed with two small pieces of glass on their top using a thermoplastic tape between the glass and the hole. Finally, copper adhesive tape was placed onto both the glass conductive sides to get good electrical contacts.

2.3. Characterization methods

2.3.1. Stability testing

Stability of the fabricated devices was assessed under dark and at open circuit (OC), in the bleached state. Optical and electrical measurements were conducted at regular time intervals. Each testing cycle included: a) Transmittance and I-V measurements of the initial state; b) coloration under insolation (1000 W m^{-2}) for various durations at open circuit; c) transmittance and I-V measurement of the colored state; d) bleaching under dark and short circuit (SC) conditions for the same duration as coloration; e) measurement of the transmittance of the bleached state. The devices were colored with the use of a solar simulator (Oriel 96000) with an A.M 1.5G filter and a radiation intensity of 1000 W m^{-2}. A Si photodiode (VTB8440B), calibrated with a Melles Griot 13PE001 Broad Band Power Meter, was used to measure the total incident irradiance [18]. The devices were illuminated from the TiO_2 side (anode), as shown in Figure 1.

2.3.2 Optical properties

In order to assess the optical properties of the devices during their stages of coloration in the visible, a Perkin Elmer Lambda 650 UV/VIS spectrometer was used. From the resulting transmittance spectra, the luminous

transmittance (T_{lum}) was calculated using equation 4 [17]. T_{lum} can be described as a spectral average using the sensitivity of the human eye $f(\lambda)$ in the photopic state as a weighting factor, where $T(\lambda)$ is the measured spectra as collected from the spectrometer.

$$T_{lum} = \frac{\int_{350nm}^{750nm} f(\lambda) \cdot T(\lambda) d\lambda}{\int_{350nm}^{750nm} f(\lambda) d\lambda} \quad (4)$$

Also, during coloration of the device, the variation of the optical density was calculated by equation 5 [18]:

$$\Delta OD_{col} = log\left(\frac{T_{lum,\ initial}}{T_{lum,\ colored}}\right) \quad (5)$$

$T_{lum,\ initial}$ and $T_{lum,\ colored}$ are the luminous transmittance of the initial state and colored state (after exposure to the solar simulator), respectively. ΔOD values are proportional to the extent of coloration for the device.

Photocoloration efficiency (PhCE) is used to assess coloration kinetics of the devices [22, 23]:

$$PhCE = \frac{\Delta OD_{col}}{G_T \cdot t} [cm^2 min^{-1} W^{-1}] \quad (6)$$

ΔOD_{col} is defined above, G_T is the incident irradiance to the device (in W cm^{-2}) and t is the exposure time (in min). For PhCE measurements, irradiance was received by the newly prepared PECs while being at their fully transparent or initial state using the solar simulator (1000 W m^{-2}) for various time intervals of 0.5, 1, 1.5, 2, 3, 6 min, and even up to 12 or 20 min if needed. After each stage of illumination, the transmittance spectra were measured.

2.3.3 Electrical properties

Characteristic I-V curves of the PEC devices were taken using the aforementioned Oriel simulator in conjunction with a Keithley 236 source meter. I-V curves were taken before and after coloration of the devices. During the initial day of fabrication of the device, I-V curves were taken after full coloration to avoid unnecessary coloration before transmittance measurements. The power conversion efficiency of the P/V element is given by [24]:

$$n = \frac{V_{mp} \cdot J_{mp}}{G_T} \quad (7)$$

where V_{mp} and J_{mp} are the voltage and current density values, respectively, that correspond to the point of maximum power, while G_T is the incident irradiance. Furthermore, fill factor (FF) is a measure of the "squareness" of the J-V curve and is given by [24]:

$$FF = \frac{V_{mp} \cdot J_{mp}}{V_{oc} \cdot J_{sc}} \quad (8)$$

where V_{oc} and J_{sc} are the open-circuit voltage and short-circuit current density, respectively. The dimensions of the PV units in the current work are 2 cm × 0.6 cm. For proper calculation of the electrical characteristics of the devices, I-V measurements were taken using a black mask, which covered the active surface of the device apart from an aperture with dimensions of 1.0 cm × 0.57 cm, placed at the center of the TiO_2 surface. The surface area was 0.57 cm^2 and current densities were calculated according to this area. The scan took place with a direction from OC to SC, at time intervals of 20 ms between each successive data point. We did not observe any hysteresis phenomena upon reversal of the scan direction.

3. Results and discussion

3.1 Performance and stability of PEC devices

The results shown in Figures 2 and 3 are referred to a PEC device with the following configuration: FTO/WO_3 (620 nm)/TiO_2 (4 µm)/MK2 20% area/Cobalt electrolyte/Pt/FTO, namely "device-1" hereafter.

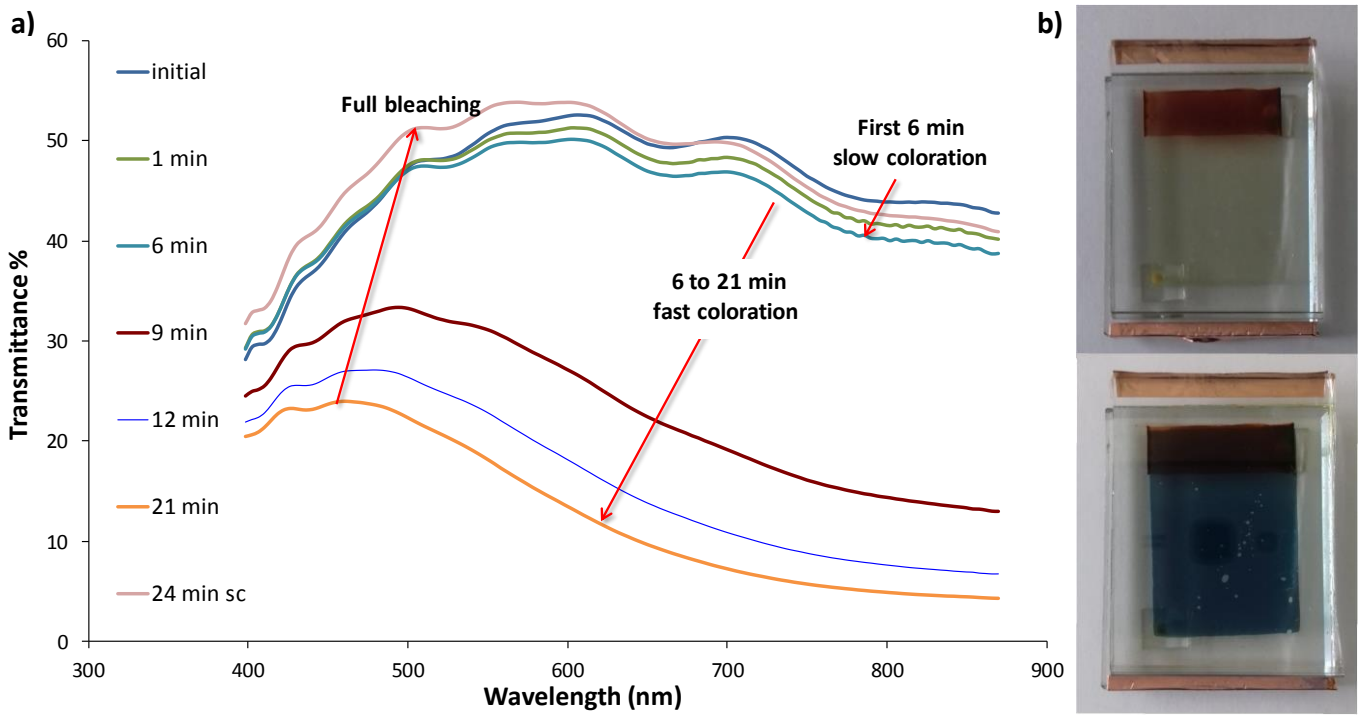

Figure 2: a) Transmittance spectra for coloration-bleaching of device-1 under illumination of 1000 W m^{-2} (AM 1.5G); b) Digital pictures of device-1 in the bleached and colored states.

As can be seen in the digital pictures shown in Figure 2, dye loading seems homogeneous and sufficiently thick (the TiO_2 film has turned red), the electrolyte is almost transparent (T_{lum} = 50%). The optical modulation is poor during the first 6 min of exposure and, then, it suddenly improves. After 21 min of exposure, a contrast ratio of about 2.9:1 is achieved, likely ascribed to the lack of Co^{3+} species. It is thus assumed that it takes 6 min of illumination under OC to form enough Co^{3+} through the reaction shown in equation 2, useful to enable proper operation of the PV element. Full bleaching is possible after 24 min under short circuit, as can be seen in Figure 2. The sample was also measured the second day after fabrication. In this case, the initial delay of 6 min was not observed. However, only a reduced contrast ratio of 1.5:1 was achieved. Furthermore, the device transparency increased (T_{lum} = 57 %), and full bleaching was possible.

PhCE plots are shown in Figure 3a, where it can be seen that the PhCE values of the aforementioned device immediately post fabrication appeared slow at first, and then increased over time. Figure 3a, also compares the PhCE plots of a device assembled with iodine electrolyte and of a device with a 1:10 dilute cobalt electrolyte. The former exhibited higher PhCE, as the PV element had a higher power conversion efficiency (in the order of 1%). The latter demonstrated lower performance, due to the low concentration of Li ions (e.g., 0.05 M) caused by dilution. The J-V plots of the PV element of device-1 are shown in Figure 3b and Table 1. The as prepared device showed a very poor performance, while - as the electrolyte composition changed - V_{OC}, I_{SC}, FF and efficiency increased and remained at the same level up to the 6th day post fabrication. The performance further improved 15 days after fabrication. The global electrical characteristics are listed in Table 1. The low power conversion efficiency observed therein can be attributed to the non-optimum characteristics of the TiO_2 film. Indeed, in order

to achieve efficient solar cells, a series of treatments of the TiO_2 anode is required. These are: annealing at 500°C to remove solvents and to improve the electrical connection of nanoparticles with the substrate [5-9, 13], immersion in an aqueous $TiCl_4$ solution at 70°C to prevent recombination at the TiO_2/electrolyte interface [6-9], use of ultra-thin compact films to prevent the contact of electrolyte with the underlying FTO electrode [5] and the use of "light scattering" layers with higher particle sizes (above 100nm) to improve light harvesting [6-9, 13]. However, these treatments involve repeated high temperature processing and use of aggressive chemicals that would degrade the sensitive WO_3 film placed beneath TiO_2. They were avoided, as explained in section 2.2.4. Thus, the resulting solar cells, seem to exhibit significant charge recombination losses, as can be verified by the low J_{SC} values. It is well known that increased recombination losses in DSSCs have an adverse effect on the V_{OC} values, which tend to decrease, as a result of a downward shift of the TiO_2 Fermi level (shown in figure 1), brought about by the reduced electron density within the semiconductor [7]. Thus, the lower than expected V_{OC} values observed in figure 3b and Table 1, can be attributed to the enhanced recombination losses.

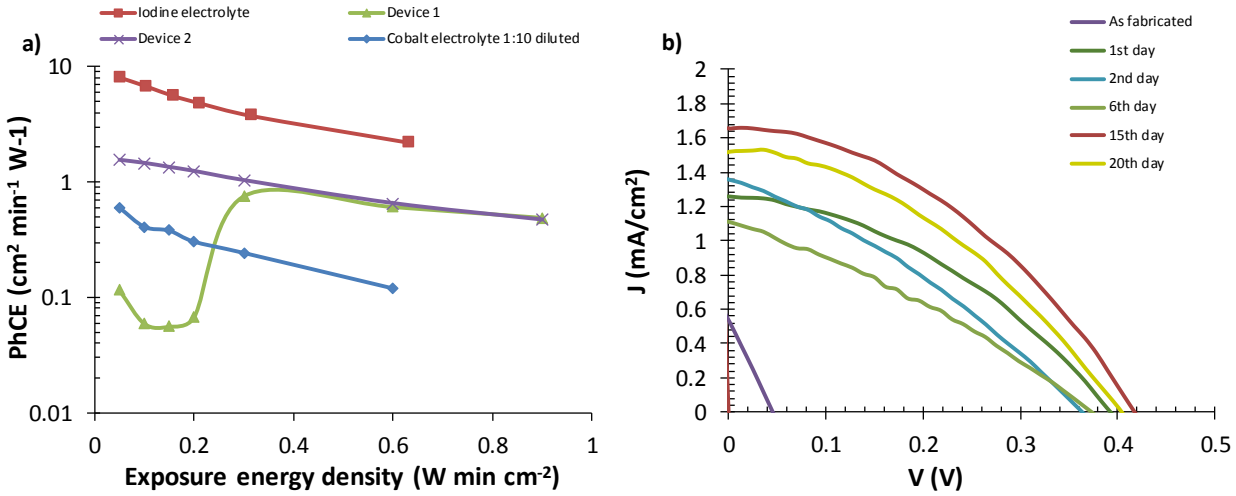

Figure 3: a) Photo-coloration efficiency of two PEC devices with MK2 dye and cobalt electrolyte (devices 1 and 2) and comparison with a similar device assembled with N719 and iodine electrolyte and with a device containing the 1:10 dilute cobalt electrolyte; b) J-V curves of device-1 (in the bleached state, at different days after fabrication), under illumination at 1000 W m^{-2} (AM 1.5G).

Table 1. Electrical characteristics of device-1 (P/V measured area = 0.57 cm^2, G = 1000 W m^{-2}).

Day of measurement	J_{SC} (mA cm^{-2})	V_{OC} (V)	FF	η %
1	1.26	0.39	0.38	0.19
2	1.36	0.36	0.32	0.16
6	1.11	0.37	0.31	0.13
15	1.65	0.42	0.40	0.28
20	1.52	0.40	0.38	0.24

In order to confirm the above results, and to investigate the slow coloration kinetics at the initial stages, a second PEC device (to be called "device-2" hereafter) was fabricated and tested. Its configuration was: FTO/WO_3 (500 nm)/TiO_2 (3 μm)/MK2 20% area/Cobalt electrolyte/Pt/FTO. Since the electrolyte initially contained only the (reduced) Co^{2+} specie of the redox couple, device-2 was exposed for 3 min at 1000 W m^{-2} prior to measurements, until a slight change in its transmittance was observed, indicating that Co^{3+} formed through the dye regeneration

process. Subsequently, the device was bleached by SC for 3 min and PhCE measurements were conducted, as described in Section 2.3.2. As can be seen in Figure 3a, the above treatment improved the PhCE of device 2 on the left side of the plot. However, upon exposure at energy densities higher than 0.4 W min cm^{-2}, the two devices demonstrated almost similar performance, without noticeable differences. Figure 4a shows the T_{lum} values of the initial, fully colored and bleached states versus days post fabrication, for device-2. Between each measurement, the device was kept at OC in a dark room. One can observe a gradual increase in the $T_{lum,initial}$ value (the device became more transparent) and a large reduction in $T_{lum,colored}$, that revealed a rapid degradation of the device, as the coloration depth was reduced to a contrast ratio of 1.1:1, 20 days after its fabrication. The device demonstrated almost full reversibility, as $T_{lum,bleach}$ matched or even exceeded $T_{lum,initial}$. Figure 4b shows a similar plot for a device assembled with an iodine-based electrolyte, which demonstrated a longer transitional period of 127 days after its fabrication before stabilizing to a contrast ratio of 1.5:1 [21]. This gradual decrease of coloration depth was attributed to the loss of photoelectrons at the WO_3/electrolyte interface through a reaction similar to that written in equation 3. This reaction was energetically more favorable than that reported as equation 1, thus it took place before Li_xWO_3 was formed, leading to the reduction of the number of coloration centers in the bulk of the EC film [21]. Gradual wetting of WO_3 by the electrolyte enhanced the loss mechanism.

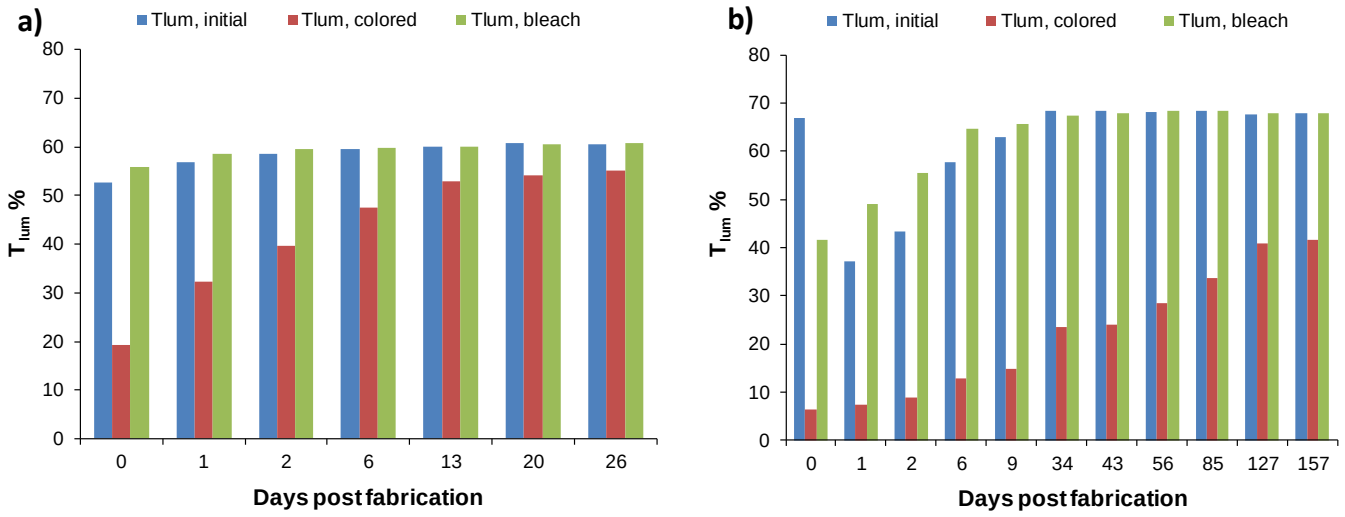

Figure 4. a) T_{lum} values on different days post fabrication for device-2; b) the same plot for a device assembled with an iodine-based electrolyte [21].

As can be seen in Figure 4, the device with the cobalt electrolyte lost coloration depth more quickly compared to that of the iodine-based PEC device. This is due to the different redox mechanism between the two couples. It is known that transition-metal redox couples like ferrocene/ferrocenium are described by kinetically fast one-electron transition from the oxidant to the reductant species and *vice versa* [5]. For this reason, the enhanced recombination rate of electrons made them unsuitable for PEC incorporation. Cobalt(II/III) complexes require a rather high energy of 1 eV for transition of Co^{2+}, which has high spin, to the low spin Co^{3+}. For this reason, $Co^{2+/3+}$ complex is characterized by slow electron kinetics and could be used as an alternative to redox standard Iodide/Triiodide [5]. However, the iodine-based redox couple shows even slower self-exchange electron kinetics compared to $Co^{2+/3+}$ because the transition between I^- to I_3^- has been described as a two-electron transfer [24]. As a result, faster recombination of the Co^{3+} species in the electrolyte with photoelectrons in the conduction band of WO_3 resulted in shorter stabilization periods.

3.2 Suppression of loss currents with the use of a barrier layer

In a previous work [21], the problem of gradual loss of coloration in PEC devices was addressed by the use of ZnS barrier layers. ZnS was found to be a suitable barrier material, as its conduction band is higher than that of WO_3 by 1.5 eV [25]. As a result, it creates a significant energy barrier preventing electrons from the WO_3 conduction band to be inserted into the electrolyte. Furthermore, it has a refractive index similar to that of WO_3 [26].

A PEC device with a configuration FTO/WO_3 (500 nm)/$\begin{Bmatrix} TiO_2(5\ \mu m)/MK2\ ,\ 20\%\ area \\ ZnS\ (35\ nm),\ 80\%\ area \end{Bmatrix}$/Cobalt electrolyte/Pt/FTO was fabricated and tested in order to assess the effect of the ZnS barrier. It will be called "device-3" hereafter. The device was stored in the dark at open circuit conditions to enable a direct comparison with corresponding ZnS-free PECs.

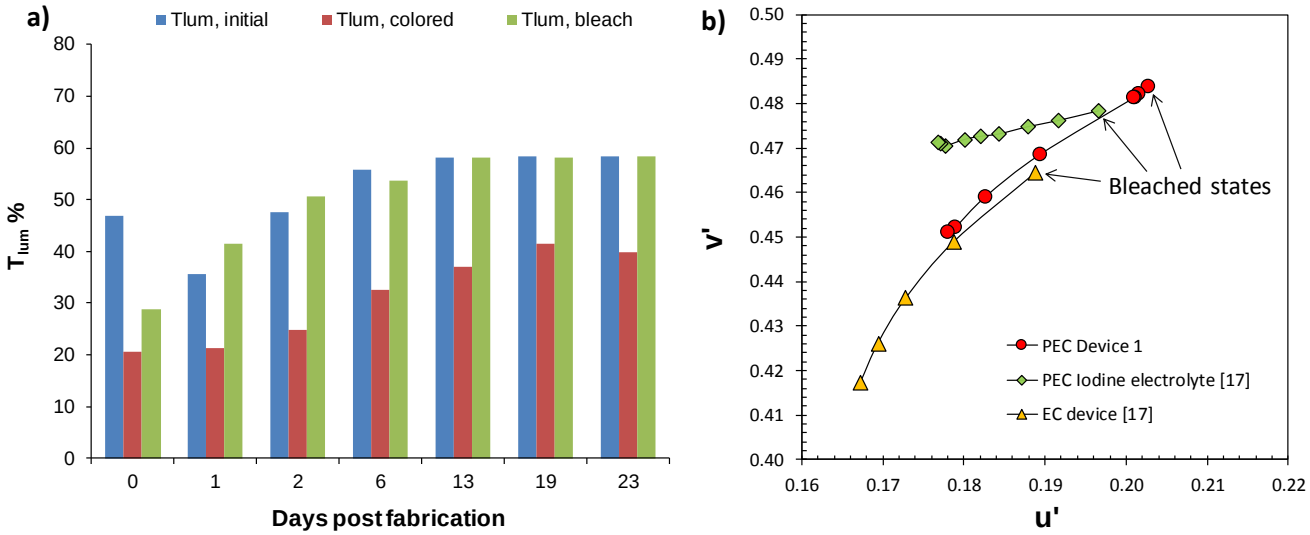

Figure 5: a) T_{lum} values for the initial, colored, bleached states versus days after fabrication for the PEC device-3 with the ZnS barrier; b) CIE 1976 UCS chromaticity diagram of PEC device-1 at various stages of coloration and comparison with an iodine electrolyte PEC and an electrochromic device.

Fig. 5a shows the luminous transmittance values for the initial, colored and bleached states for the PEC device-3 with the ZnS barrier. The contrast ratio of the device during its initial day of fabrication was 2.3:1, slightly lower than that of the devices without ZnS. The device became fully reversible 13 days after its fabrication. Furthermore, the stabilization of the coloration depth was achieved 19 days after fabrication with a contrast ratio of 1.5:1. The value of the stabilized contrast ratio of device-3 definitely represents an improvement on the stability of cobalt-based PECs, confirming the effective role of ZnS barrier.

3.3 Color coordinates

Fig. 5b shows the chromaticity diagrams of the PEC device-1 and of the corresponding PEC device with iodine electrolyte, also compared with a typical electrochromic device (both taken from reference [17]), at various coloration stages. These diagrams are plotted accordingly to the CIE 1976 UCS chromaticity system. The color coordinates (u', v') are defined as follows:

$$u' = \frac{4X}{X+15Y+3Z}, \quad v' = \frac{9Y}{X+15Y+3Z} \tag{9}$$

with *X, Y, Z* the Tristimulus values [27], calculated using the CIE 1931 2-degree observer color matching functions. Comparison of the two PEC devices reveals different colorations, disregarding their similar layout. As can be inferred from the color coordinates of Fig. 5b, for the coloration of device-1, both u' and v' decrease and, as a result, the device color becomes blue (see also the photographs in Figure 2). During coloration of the PEC device with iodine electrolyte, the u' coordinate undergoes the most significant changes and, as a result, the device assumes a bluish-green color. This difference can be attributed to the different electrolytes used. Indeed, the iodine-based electrolyte contains small quantities of I_2 (0.0025 M), [17] which absorbs in the red region of the spectra, giving a slightly yellow tint to the resulting solution, while cobalt complexes are weak light absorbers in the visible region [7], as can be seen in figure S1. Furthermore, the color coordinates of device-1 resemble those of a typical electrochromic device (with transparent electrolyte) during coloration. This is an advantage of the use of cobalt-based electrolytes in PECs, since the blue color of Li_xWO_3 in electrochromic windows has gained significant acceptance among users [4].

Conclusions

As follows from the results reported in this work, we have proven for the first time the fabrication of partly covered photoelectrochromic devices with cobalt-based electrolytes, which were successfully tested. Their configuration is: FTO/WO_3/TiO_2 sensitized by the MK2 dye (20% area)/Cobalt electrolyte/Pt/FTO.

These devices exhibited rather good transparency in the bleached state, with a T_{lum} value above 50 %, and coloration speeds in the order of minutes, with a maximum contrast ratio of 2.9:1 after 21 min of illumination at 1000 W m^{-2} under open circuit conditions. They showed reversibility, as they could be fully bleached in short circuit conditions. The maximum measured power conversion efficiency was 0.28 %, rather low but well sufficient to drive the coloration process. The low efficiency values are due to limitations imposed by conflicting requirements of the photovoltaic and electrochromic elements. Moreover, prior to measurements, an initial "treatment" of the devices consisting in their illumination under open circuit conditions for 3 min at 1000 W m^{-2}, was needed in order to form the Co^{3+} cation, which was not present initially in the electrolyte solution. The higher recombination losses of the $Co^{2+/3+}$ redox shuttle compared to I^-/I_3^- led to a considerable reduction in coloration depth 20 days post fabrication, due to loss of photoelectrons at the WO_3/electrolyte interface. Remarkably, the use of a 35 nm thick ZnS barrier deposited on top of WO_3 suppressed these losses, achieving a stabilized contrast ratio of 1.5:1, 23 days post fabrication.

The color coordinates of the present devices resemble those of typical electrochromics (viz., they both exhibit blue coloration), as a result of the absence of the absorbing iodine in the electrolyte that produces a green tint upon coloration. Further work is necessary in order to improve both their photovoltaic and optical performance, but the results reported in his work enlighten the promising prospects of the newly developed devices for smart energy-saving applications.

Acknowledgments

K. Theodosiou acknowledges the financial support from the Greek State Scholarship Foundation (IKY) through the Action: "Scholarships program for second-stage postgraduate studies" (Grant Number: 2017-050-0504-10281) of the Operational Program "Development of human resources.

Data Availability

The raw data required to reproduce these findings are available to download from the Mendeley Data repository. The processed data required to reproduce these findings are available to download from the Mendeley Data repository.

References

[1] Marco Casini, "Active dynamic windows for buildings: A review", Renewable Energy 119 (2018) 923-934

[2] C.G. Granqvist, M.A. Arvizu, I. Bayrak Pehlivan, H.-Y. Qu, R.-T. Wen, G.A. Niklasson, "Electrochromic materials and devices for energy efficiency and human comfort in buildings: A critical review", Electrochimica Acta 259 (2018) 1170-1182

[3] Aritra Ghosh, Brian Norton, "Advances in switchable and highly insulating autonomous (self-powered) glazing systems for adaptive low energy buildings", Renewable Energy 126 (2018) 1003-1031

[4] A. Cannavale, P. Cossari, G. E. Eperon, S. Colella, F. Fiorito, G. Gigli, H. J. Snaith and A. Listorti, "Forthcoming Perspectives of Photoelectrochromic Devices: A critical review", Energy Environ. Sci., 9, (2016), 2682-2719.

[5] Lingamallu Giribabu, Ramababu Bolligarla, Mallika Panigrahi, "Recent advances of Cobalt (II/III) redox couples for Dye-sensitized solar cell appilications." The Chemical Record 15 Issue 4 (2015) 760-788.

[6] Zhihui Wang, Lihai Miu, Huiyun Yao, Mao Liang, Suhao Yan, Jiawei Wang, Tao Guo, Lijing Zhang, Jing Chen, Song Xue, "Organic sensitizers featuring 9H-thieno[2',3':4,5]thieno[3,2-b]thieno[2',3':4,5]thieno[2,3-d]pyrrole core for high performance dye-sensitized solar cells", Dyes and Pigments 162 (2019) 126–135

[7] Kitty Y. Chen, Phil A. Schauer, Brian O. Patrick and Curtis P. Berlinguette, "Correlating cobalt redox couples to photovoltage in the dye-sensitized solar cell", Dalton Transactions 47 (2018) 11942-11952

[8] Liang Xu, Chenghao Xin, Chen Li, Wenjun Wu, Jianli Hua, Weihong Zhu, "Custom-designed metal-free quinoxaline sensitizer for dye-sensitized solar cells based on cobalt redox shuttle" Solar Energy 169 (2018) 450–456

[9] Yoon Jun Son, Jin Soo Kang, Jungjin Yoon, Jin Kim, Juwon Jeong, Jiho Kang, Myeong Jae Lee, Hyun S. Park, Yung-Eun Sung, "Influence of TiO2 Particle Size on Dye-Sensitized Solar Cells Employing an Organic Sensitizer and a Cobalt(III/II) Redox Electrolyte", J. Phys. Chem. C 2018, 122, 7051−7060

[10] Josh Baillargeon, Yuling Xie, Austin L. Raithel, Behnaz Ghaffari, Richard J. Staples, Thomas W. Hamann, "Spin-Doctoring Cobalt Redox Shuttles for Dye-Sensitized Solar Cells", Inorg. Chem. 2018, 57, 11633−11645

[11] Imperiyka, M., Ahmad, A., Hanifah, S.A., Bella, F. "A UV-prepared linear polymer electrolyte membrane for dye-sensitized solar cells" Physica B: Condensed Matter (2014), 450, 151-154.

[12] Shanti, R., Bella, F., Salim, Y.S., Chee, S.Y., Ramesh, S., Ramesh, K. "Poly(methyl methacrylate-co-butyl acrylate-co-acrylic acid): Physico-chemical characterization and targeted dye sensitized solar cell application", Materials and Design (2016) , 108, 560-569.

[13] Simon Mathew, Aswani Yella, Peng Gao, Robin Humphry-Baker, Basile F. E. Curchod, Negar Ashari-Astani, Ivano Tavernelli, Ursula Rothlisberger, Md. Khaja Nazeeruddin, Michael Gratzel, "Dye-sensitized solar cells with 13% efficiency achieved through the molecular engineering of porphyrin sensitizers", Nature Chemistry (2014) 6, 242-247

[14] Antonio Carella, Fabio Borbone and Roberto Centore, "Research Progress on Photosensitizers for DSSC", Frontiers in Chemistry 6(2018) article 481

[15] Eri Amasawa, Naoki Sasagawa, Mutsumi Kimura, Minoru Taya, "Design of a New Energy-Harvesting Electrochromic Window Based on an Organic Polymeric Dye, a Cobalt Couple, and PProDOT-Me2", Adv. Energy Mater. 4 (2014) 1400379

[16] Xingming Wu, Jianming Zheng, Gui Luo, Dan Zhu, Chunye Xu, "Photoelectrochromic devices based on cobalt complex electrolytes" RSC Advances 6 (2016) 81680–81684

[17] G. Leftheriotis, G. Syrrokostas, P. Yianoulis ''Partly covered photoelectrochromic devices with enhanced coloration speed and efficiency", Solar Energy Materials & Solar Cells 96 (2012) 86–92.

[18] G. Syrrokostas , G. Leftheriotis, P. Yianoulis, Performance and stability of "partly covered" photoelectrochromic devices for energy saving and power production, Solid State Ionics 277 (2015) 11–22.

[19] G. Leftheriotis, M. Liveri, M. Galanopoulou, I.D. Manariotis, P. Yianoulis "A simple method for the fabrication of WO_3 films with electrochromic and photocatalytic properties" Thin Solid Films 573 (2014) 6–13.

[20] G. Syrrokostas, M. Giannouli, P. Yiannoulis, "Effects of paste storage on the properties of nanostructured thin films for the development of dye-sensitized solar cells", Renewable Energy 34 (2009) 1759-1764

[21] A. Dokouzis, K. Theodosiou, G. Leftheriotis, "Assessment of the long-term performance of partly covered photoelectrochromic devices under insolation and in storage", Solar energy materials and solar cells 182 (2018) 281-293

[22] G. Leftheriotis, G. Syrrokostas, P. Yianoulis "Photocoloration efficiency and stability of photoelectrochromic devices" Solid State Ionics 231 (2013) 30–36.

[23] G. Leftheriotis, G. Syrrokostas, P. Yianoulis, "Development of photoelectrochromic devices for dynamic solar control in buildings", Solar Energy Materials & Solar Cells 94 (2010) 2304–2313.

[24] A. Hagfeldt, G. Boschloo, L. Sun, L. Kloo, H. Pettersson, "Dye-Sensitized Solar Cells", Chemical Reviews 110 (2010) 6595–6663.

[25] A. Kudo and Y. Miseki, "Heterogeneous photocatalyst materials for water splitting" Chem. Soc. Rev. 38 (2009) 253-278

[26] J.M. Siqueiros, R. Machorro, L.E. Regalado, "Determination of the optical constants of MgF2 and ZnS from spectrophotometric measurements and the classical oscillator method", Applied Optics 27 (1988) 2549–2553

[27] R.W.G. Hunt, M.R. Pointer, Measuring Colour, 4th ed., John Wiley and Sons Ltd., UK, 2011, pp. 19–41(Chapter 2)

Figure captions

Figure 1: Scheme of "party covered" PEC device: a) coloration process; b) bleaching process.

Figure 2: a) Transmittance spectra for coloration-bleaching of device-1 under illumination of 1000 W/m2 (AM 1.5G); b) Digital pictures of device 1 in the bleached and colored states.

Figure 3: a) Photo-coloration efficiency of two PEC devices with MK2 dye and cobalt electrolyte (devices 1 and 2) and comparison with a similar device assembled with N719 and iodine electrolyte and with a device containing the 1:10 dilute cobalt electrolyte; b) J-V curves of device-1 (in the bleached state, at different days after fabrication), under illumination at 1000 W/m2 (AM 1.5G).

Figure 4: a) Tlum values on different days after fabrication for device-2; b) The same plot for a device assembled with an iodine-based electrolyte [19].

Figure 5: a) Tlum values for the initial, colored, bleached states versus days after fabrication for the PEC device-3 with the ZnS barrier; b) CIE 1976 UCS chromaticity diagram of PEC device-1 at various stages of coloration and comparison with an iodine electrolyte PEC and an electrochromic device.

Table captions

Table 1: Electrical characteristics of device-1. (P/V measured area= 0.57 cm^2. G= 1000 Wm^{-2}).

Figure 1

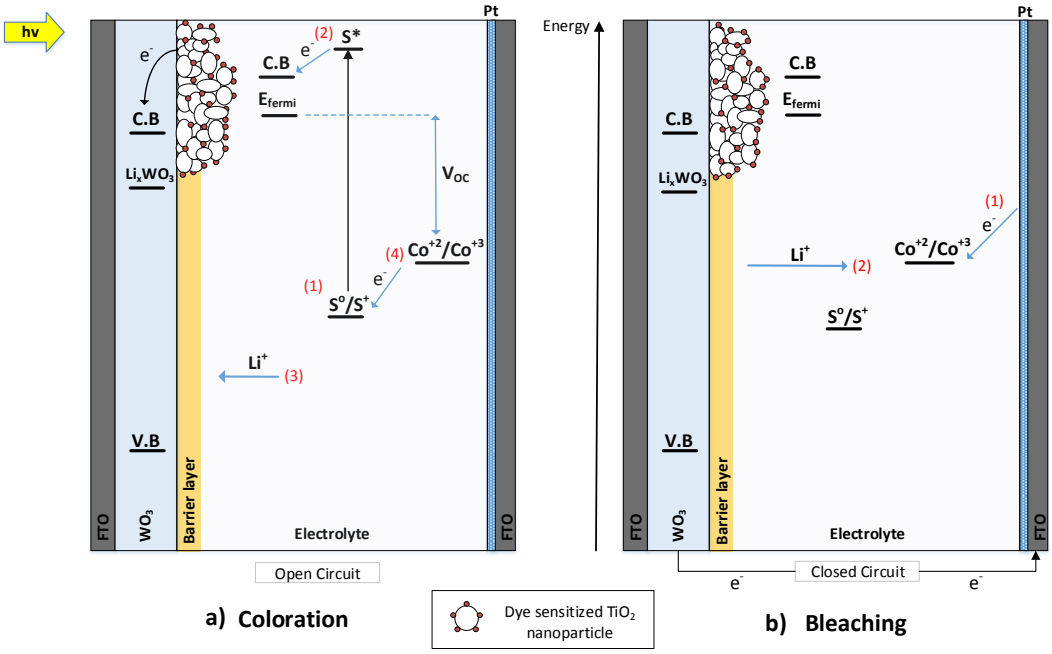

Figure 1: Scheme of "partly covered" PEC device: a) coloration, and b) bleaching process.

Figure 2

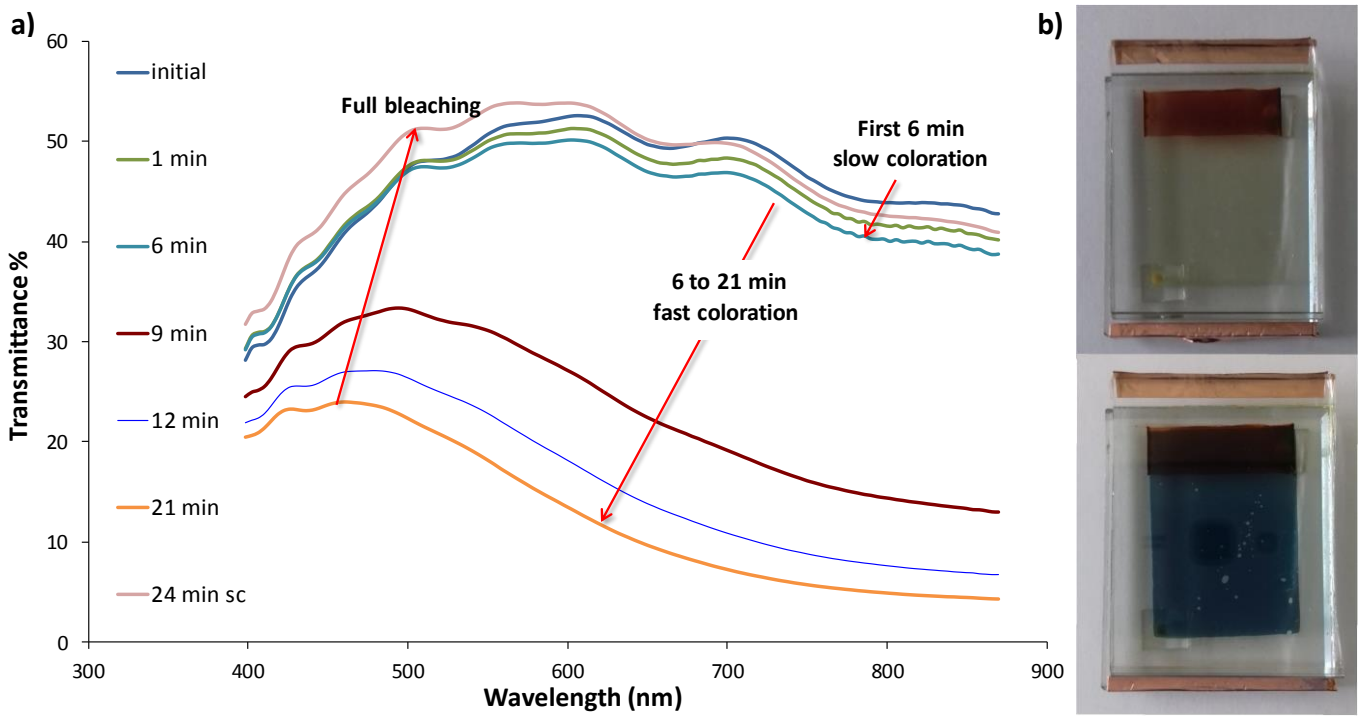

Figure 2: a) Transmittance spectra for coloration-bleaching of device-1 under illumination of 1000 W m^{-2} (AM 1.5G); b) Digital pictures of device-1 in the bleached and colored states.

Figure 3

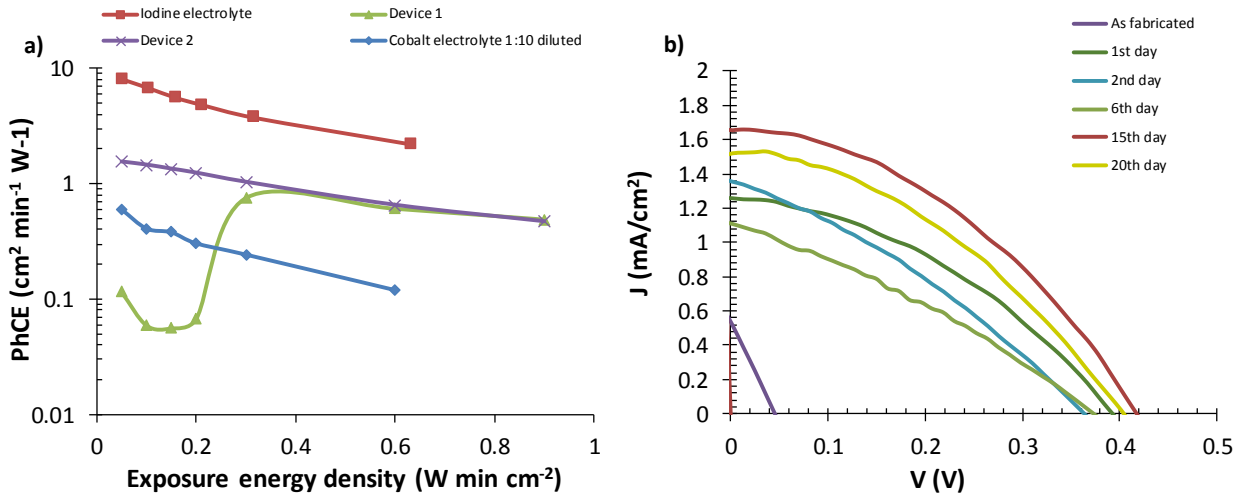

Figure 3: a) Photo-coloration efficiency of two PEC devices with MK2 dye and cobalt electrolyte (devices 1 and 2) and comparison with a similar device assembled with N719 and iodine electrolyte and with a device containing the 1:10 dilute cobalt electrolyte; b) J-V curves of device-1 (in the bleached state, at different days after fabrication), under illumination at 1000 W m^{-2} (AM 1.5G).

Figure 4

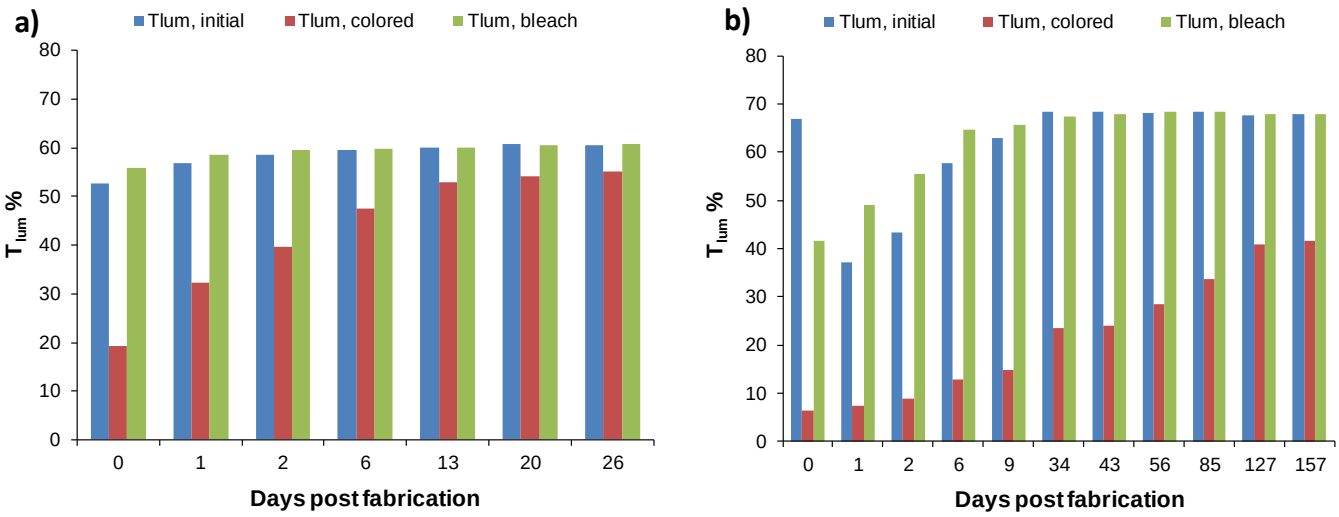

Figure 4. a) T_{lum} values on different days post fabrication for device-2; b) the same plot for a device assembled with an iodine-based electrolyte [21].

Figure 5

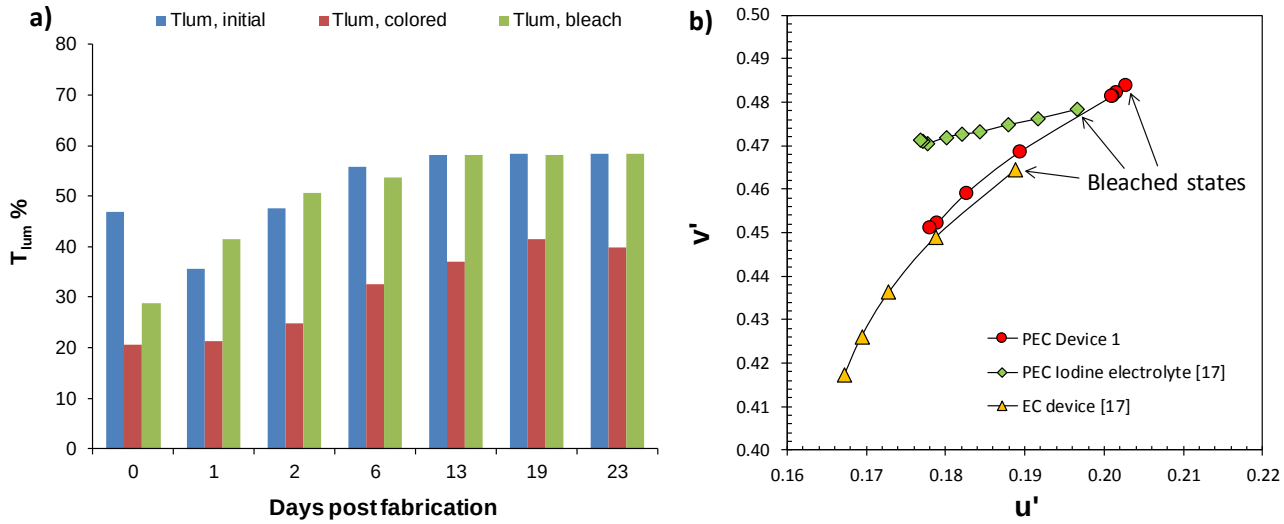

Figure 5: a) T_{lum} values for the initial, colored, bleached states versus days after fabrication for the PEC device-3 with the ZnS barrier; b) CIE 1976 UCS chromaticity diagram of PEC device-1 at various stages of coloration and comparison with an iodine electrolyte PEC and an electrochromic device.